Epigenetic Inactivation of Galanin Receptor 1 in Head and Neck Cancer

Kiyoshi Misawa,[1,2] Yo Ueda,[1,2] Takeharu Kanazawa,[1,3] Yuki Misawa,[1,2] Ilwhan Jang,[1,4] John Chadwick Brenner,[1] Tetsuya Ogawa,[1,5] Satoru Takebayashi,[1,2] Reidar A. Grenman,[6] James G. Herman,[7] Hiroyuki Mineta,[2] and Thomas E. Carey[1]

Abstract

Purpose: One copy of the galanin receptor 1 (*GALR1*) locus on 18q is often deleted and expression is absent in some head and neck squamous cell carcinoma (HNSCC) cell lines. To determine if loss of heterozygosity and hypermethylation might silence the *GALR1* gene, promoter methylation status and gene expression were assessed in a large panel of HNSCC cell lines and tumors.

Experimental Design: Promoter methylation of *GALR1* in 72 cell lines and 100 primary tumor samples was analyzed using methylation-specific PCR. GALR1 expression and methylation status were analyzed further by real-time PCR and bisulfite sequencing analysis.

Results: The *GALR1* promoter was fully or partially methylated in 38 of 72 (52.7%) HNSCC cell lines but not in the majority 18 of 20 (90.0%) of nonmalignant lines. *GALR1* methylation was also found in 38 of 100 (38%) primary tumor specimens. Methylation correlated with decreased *GALR1* expression. In tumors, methylation was significantly correlated with increased tumor size ($P = 0.0036$), lymph node status ($P = 0.0414$), tumor stage ($P = 0.0037$), *cyclin D1* expression ($P = 0.0420$), and *p16* methylation ($P = 0.0494$) and survival ($P = 0.045$). Bisulfite sequencing of 36 CpG sites upstream of the transcription start site revealed that CpG methylation within transcription factor binding sites correlated with complete suppression of *GALR1* mRNA. Treatment with trichostatin A and 5-azacytidine restored *GALR1* expression. In UM-SCC-23 cells that have total silencing of *GALR1*, exogenous *GALR1* expression and stimulation with galanin suppressed cell proliferation.

Conclusions: Frequent promoter hypermethylation, gene silencing, association with prognosis, and growth suppression after reexpression support the hypothesis that *GALR1* is a tumor suppressor gene in HNSCC.

Authors' Affiliations: [1]Laboratory of Head and Neck Cancer Biology, Comprehensive Cancer Center, Otolaryngology/Head and Neck Surgery, University of Michigan, Ann Arbor, Michigan; [2]Otolaryngology/Head and Neck Surgery, Hamamatsu University School of Medicine, Shizuoka, Japan; [3]Otolaryngology, Head and Neck Surgery, Jichi University School of Medicine, Saitama, Japan; [4]Otolaryngology/Head and Neck Surgery, Ghil Hospital, Incheon, Korea; [5]Aichi Cancer Center, Nagoya, Japan; [6]Otolaryngology/Head and Neck Surgery, Turku University Central Hospital, Turku, Finland; and [7]Sidney Kimmel Comprehensive Cancer Center at Johns Hopkins, Baltimore, Maryland

Received 11/1/07; revised 5/28/08; accepted 6/30/08.

Grant support: NIH/National Institute of Dental and Craniofacial Research grant 5 R01 DE12477 (T.E. Carey) and NIH/National Cancer Institute through the University of Michigan Head and Neck SPORE grant 1 P50 CA97248, Cancer Center Support grant 5 P30 CA46592, and NIH/National Institute of Dental and Craniofacial Research Center Core grant P30 DC05188.

The costs of publication of this article were defrayed in part by the payment of page charges. This article must therefore be hereby marked *advertisement* in accordance with 18 U.S.C. Section 1734 solely to indicate this fact.

Note: Supplementary data for this article are available at Clinical Cancer Research Online (http://clincancerres.aacrjournals.org/).

Requests for reprints: Thomas E. Carey, Laboratory of Head and Neck Cancer Biology, Comprehensive Cancer Center, Otolaryngology/Head and Neck Surgery, University of Michigan, 1150 West Medical Center Drive, Room 5311, Medical Sciences I, Ann Arbor, MI 48109-5616. Phone: 734-764-4371; Fax: 734-764-0014; E-mail: careyte@umich.edu.

doi:10.1158/1078-0432.CCR-07-4673

Loss of heterozygosity (LOH) on chromosome 18q in head and neck squamous cell carcinoma (HNSCC) is associated with significantly decreased survival (1). Galanin receptor 1 (*GALR1*), a G-protein-coupled receptor (GPCR) that maps to the commonly lost 18q23 region (2), exhibits aberrant expression in HNSCC cells with 18q LOH. Loss of one copy and inactivation of the remaining *GALR1* gene would be consistent with it acting as a tumor suppressor gene. Abnormalities affecting GPCRs have been implicated in many human tumors (3–5). Similarly, there is a growing literature implicating a variety of GPCR signaling pathways in head and neck cancer (6–14). *GALR1* and its ligand, galanin, are expressed in normal keratinocytes, suggesting that loss of *GALR1* plays a role in the development or progression of HNSCC (15). Furthermore, we found two cell lines with *GALR1* mutations that affect the sixth transmembrane domain, a region known to affect GPCR function (15).

There are three galanin receptors: *GALR1*, *GALR2* (17q25.3), and *GALR3* (22q13.1; ref. 16). Galanin activates the receptors and initiates signal transduction (17). *GALR1* is reported to couple to heterotrimeric G proteins of the G_i type, which inhibit cyclic AMP (16). Galanin regulates many physiologic functions in mammals (15, 18) and may have a role in

Translational Relevance

Identifying biomarkers of those tumors that will progress and cause the death of the patient is a critical area of research, particularly if the biomarker can be linked to targeted therapy. We showed previously that loss of chromosome 18q23 was associated with poor survival in head and neck cancer and found that GALR1 mapped to the minimal region of loss. We postulated that GALR1 might be a tumor suppressor gene and that loss of one GALR1 copy and silencing of the other copy could promote aggressive tumor progression. In this article, we show that GALR1 promoter methylation and silencing is frequent in head and neck squamous cancers and is statistically significantly associated with decreased survival. Restoring GALR1 expression inhibits tumor cell growth. Thus, specific histone deacetylase or methyltransferase inhibitors may provide a means to target GALR1 expression in the most aggressive tumors.

Alzheimer's disease (19). *GALR2* was reported to activate $G_{12/13}$ proteins (20) that activate mitogenic cascades. However, galanin receptor function may depend on the cell type. Berger et al. (21) reported that exogenous expression of *GALR2* inhibited cell proliferation and induced apoptosis in neuroblastoma cells, whereas in the same cell type expression of *GALR1* only inhibited cell proliferation. Thus, the functions of *GALR1*, *GALR2*, and *GALR3* are not well understood. Our recent findings support a growth regulatory function for GALR1 because antibody blockade of this receptor enhances proliferation of HNSCC cells (8) and restoration of GALR1 expression inhibits cell growth and tumor formation in HNSCC cells (22). Thus, *GALR1* appears to act as a tumor suppressor in HNSCC.

Tumor suppressor genes may be inactivated by point mutations, homozygous deletions, or LOH and aberrant methylation (23). Methylation of CpG sites within promoter regions is often associated with silenced gene expression (24, 25). The *GALR1* promoter is a TATA-less promoter containing GC-rich sequences that may be susceptible to DNA methylation and gene silencing (26).

In this study, we show for the first time that loss of GALR1 expression is associated with hypermethylation of key CpG sites within transcription factor binding domains and that expression can be restored after treatment with the demethylating agent, 5-azacytidine, and the histone deacetylase inhibitor, trichostatin A (TSA). Moreover, assessment of primary tumor specimens confirmed that hypermethylation is as common in patient tumors as in cell lines and is directly associated with tumor size and metastasis. Finally, restoration of *GALR1* expression in HNSCC cells resulted growth inhibition in response to galanin stimulation, supporting the hypothesis that *GALR1* is a tumor suppressor gene.

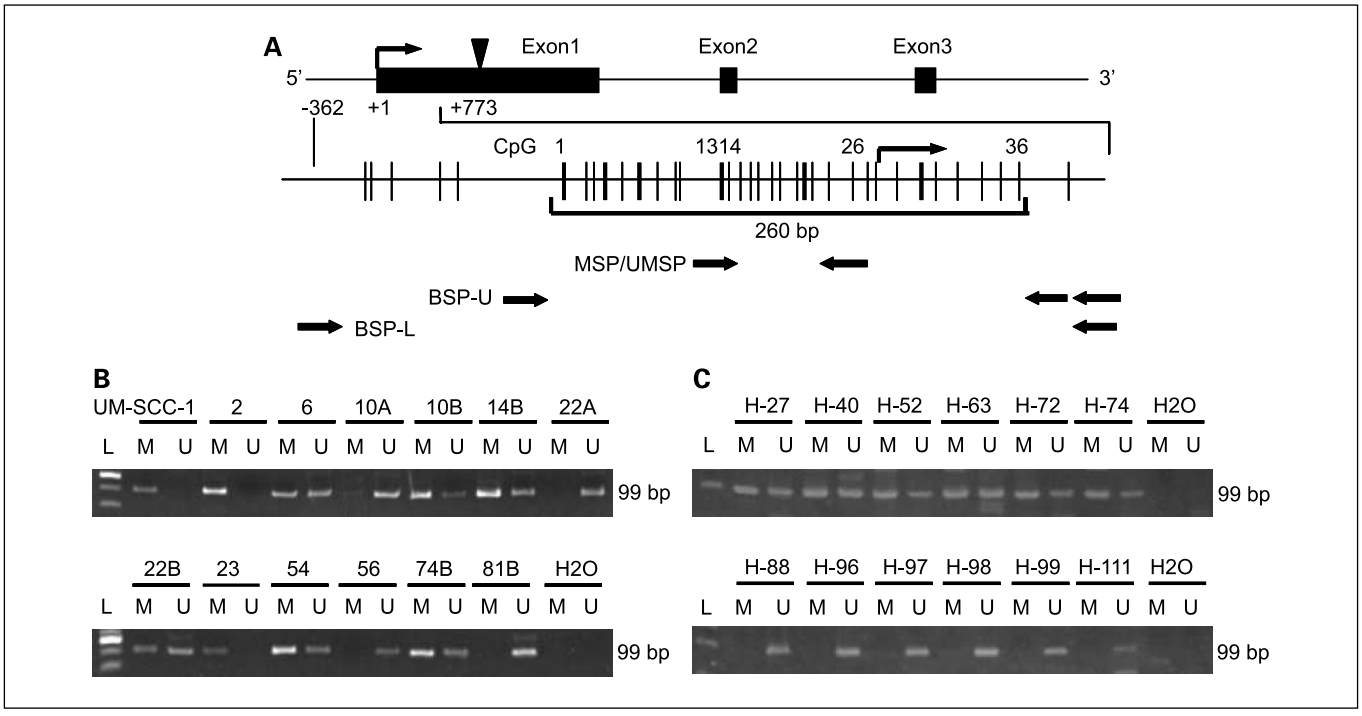

Fig. 1. Diagrammatic representation of the GALR1 gene and its proximal promoter and GALR1 methylation analysis using the MSP assay. *A,* GALR1 exon structure and CpG sites within expanded views of the promoter region relative to the transcript start site (TSS). *Vertical lines,* individual CpG sites. The *bracket* (*bottom*) encloses the 260-bp region that includes the TSS and the 36 individual CpG sites that were examined for frequency of methylation. *Straight arrows,* relative location of the primers used for methylation-specific PCR (MSP) and bisulfite sequencing; *bent arrow,* TSS; *arrowhead,* translation start site (ATG). *B,* representative examples of MSP of GALR1 in UM-SCC cell lines, showing samples that are fully methylated (UM-SCC-1, UM-SCC-2, and UM-SCC-23), partially methylated (UM-SCC-6, UM-SCC-10B, UM-SCC-14B, UM-SCC-22B, and UM-SCC-74B), or unmethylated (UM-SCC-10A, UM-SCC-22A, UM-SCC-56, and UM-SCC-81B). *C,* representative examples of MSP of GALR1 in primary tumors from Hamamatsu University Hospital, showing samples that are methylated (H-27, H-40, H-52, H-63, H-72, and H-74) or unmethylated (H-88, H-96, H-97, H-98, H-99, and H-111).

Table 1. *GALR1* gene methylation status in HNSCC primary samples

Patient and tumor characteristics (n = 100)	Methylation		P
	Present (n = 38)	Absent (n = 62)	
Age			
≥70 (29)	9	20	
<70 (71)	29	42	0.2466*
Gender			
Male (78)	27	51	
Female (22)	11	11	0.1438*
Smoking status			
Smoker (69)	26	43	
Nonsmoker (31)	12	19	0.6280*
Tumor site			
Oral cavity and oropharynx (45)	14	31	
Others (55)	24	31	0.1407*
Tumor size			
T_1 (10)	2	8	
T_2 (39)	9	30	
T_3 (19)	10	9	
T_4 (32)	17	15	0.0036** †
Lymph node status			
N_0 (44)	11	33	
N_1 (22)	11	11	
N_2 (27)	13	14	
N_3 (7)	3	4	0.0414* †
Stage			
I (6)	2	4	
II (22)	3	19	
III (17)	5	12	
IV (55)	28	27	0.0037** †
p53 expression			
Mutant type (51)	20	31	
Wild-type (49)	18	31	0.4804*
PTEN expression			
Low (31)	13	18	
High (69)	25	44	0.3720*
Cyclin D1 expression			
High (33)	17	16	
Low (67)	21	46	0.0420**
p16 methylation			
Yes (54)	25	29	
No (46)	13	33	0.0494**
RASSF1A methylation			
Yes (22)	10	12	
No (78)	28	50	0.2831*
Overall survival			
Kaplan-Meier (%)	36.1	57.1	0.0448* ‡

*Fisher's exact probability test.
† Mann-Whitney U test.
‡ Log-rank test.

Materials and Methods

Cell lines. DNA from 72 HNSCC cell lines established from patients at either the University of Michigan (62 UM-SCC) or the University of Turku (10 UT-SCC) was used for methylation-specific PCR (MSP) analysis. The letter A after the cell line number (e.g., UM-SCC-10A) designates the primary tumor cell lines. Subsequent tumor lines from the same patients have a B designation. Fibroblasts from the original tumor specimen (15 samples) or transformed B-lymphocytes from the tumor cell line donors (3 samples) were used as the source of normal somatic DNA. Nonmalignant cells from the donors of UM-SCC and UT-SCC cell lines have the same number [e.g., UM-SCC-6 and UM-6F (fibroblasts)]. Other control cells included normal human keratinocytes (NHK) and HPV16 transformed oral keratinocytes (HOK-16B) cells (a gift from Dr. No Hee Park; ref. 27). cDNA from a normal human brain cDNA library (Invitrogen) was an additional control.

Tumor specimens. DNA was isolated from specimens obtained at surgery from 100 primary HNSCC tumors. All patients were treated at the Department of Otolaryngology, Hamamatsu University School of Medicine. Clinical information including age, sex, smoking status, tumor size, lymph node status, and stage were obtained from the clinical records. The mean age was 63.9 years (range 39-90), and the male/female ratio was 78:22. Primary tumor sites were oral cavity (n = 34), hypopharynx (n = 24), larynx (n = 20), oropharynx (n = 11), and paranasal cavity (n = 11).

Bisulfite modification. Genomic DNA was extracted using the Wizard Genomic DNA Purification Kit (Promega). Bisulfite modification of genomic DNA converts unmethylated cytidine residues to uradine residues that are then converted to thymidine during

subsequent PCR (28). Methylated cytidine residues are not altered by bisulfite treatment. In brief, 1 μg genomic DNA was denatured with NaOH (final concentration, 0.2 mol/L) and then incubated with sodium bisulfite (3 mol/L; Sigma; pH 5.0) and hydroquinone (10 mmol/L; Sigma) at 55°C for 16 h. Bisulfite-modified DNA was purified using the Wizard DNA Clean-Up System (Promega). For DNA desulfonation, NaOH (final concentration, 0.3 mol/L) was added, incubated at room temperature for 5 min, ethanol precipitated, and resuspended in 100 μL autoclaved distilled water.

Methylation analysis of the GALR1 proximal promoter. The *GALR1* exon structure and the proximal promoter are shown in Fig. 1A. An expanded view of the CpG-rich proximal promoter and exon 1 extending from -362 to +773 bp that includes both the transcription start site (TSS; bent arrow) and the start codon (black arrowhead) is shown below the exon map. The 260-bp region surrounding the TSS has 36 CpG sites. Potential transcription factor binding sites were detected within this region using TFSEARCH. Sites 13 and 14 are part of a consensus activating protein-2 (Ap-2) site and site 26 is within a consensus selective promoter factor 1 (Sp1) site.

MSP analysis. Methylation in the region near the TSS was assessed using bisulfite-treated DNA PCR amplified with MSP primers, MSP-F (5′-GGTTCGCGGTATTCGGTAGT-3′, upstream) and MSP-R (5′-TCGCCGCCCACCTCCCGACTAA-3′, downstream), and unmethylated DNA-specific primers (UMSP), UMSP-F (5′-GGTTTGTGGTATTTGG-TAGT-3′, upstream) and UMSP-R (5′-TCACCACCCACCTCCCAACTAA-3′, downstream). Arrows show the binding locations of the MSP/UMSP primers below the expanded region (Fig. 1A). The PCR conditions were 94°C for 5 min; 33 cycles at 94°C for 30 s, 60°C for 30 s, and 72°C for 40 s; and a final extension at 72°C for 5 min. The 99-bp PCR products were separated by electrophoresis through a 9% acrylamide gel and stained with ethidium bromide. To analyze the methylation status of the *p16* gene and the *RASSF1A* gene, primers and conditions as described by Herman et al. (28) and Kuroki et al. (29) were used.

Bisulfite sequencing analysis. The frequency of methylation at 36 individual CpG sites within the bracketed 260-bp region was assessed on the top or bottom strands using bisulfite-specific sequencing. Of the 36 CpG sites analyzed, numbers 1 to 27 are upstream of the TSS and numbers 28 to 36 are downstream (Fig. 1A). Bisulfite sequencing PCR (BSP) primer pairs specific for modified top and bottom strand DNAs were designed to contain no CpG sites. Top strand primers were BSP-U-F (5′-GAGGAGGAAAGGTATTAATGGATGAGGAGG-3′), BSP-U-R (5′-ACTCTTTTAAAAAACTTCCTAATAATAAAT-3′), and BSP-U-RN (5′-AATACCAAAAACTTCTCTACTACAACTAA-3′). In a second PCR, BSP-U-F and a nested primer, BSP-U-RN, were used with 0.5 μL of the PCR product as template. PCR conditions for both first and second PCR were 94°C for 5 min; 35 cycles at 94°C for 30 s, 50.8°C for 30 s, and 72°C for 50 s; and a final extension at 72°C for 7 min. The bottom strand primers were BSP-L-F (5′-AGGTTTTTTGGTGGTGGATA-3′) and BSP-L-R (5′-ACCAATTTTACAAAACTCCA-3′). The binding locations of the bisulfite sequencing primers are shown by arrows below the expanded region (Fig. 1A). The bottom strand PCR conditions were 94°C for 5 min; 40 cycles at 94°C for 30 s, 56.0°C for 30 s, and 72°C for 50 s; and a final extension at 72°C for 5 min. The PCR products were separated by electrophoresis through a 1.5% agarose gel containing ethidium bromide, extracted from the gel with the QIAquick Gel Extraction Kit (Qiagen), and cloned into pGEN T-Easy vector, and at least nine clones were sequenced by the ABI model 3730 sequencer using T7 or SP6 primers.

RNA extraction and GALR1 reverse transcription-PCR. Total RNA from 13 HNSCC cell lines, including 9 with loss of one copy of chromosome 18q, 1 with no loss of 18q, and 3 for which 18q status is unknown, was isolated using the RNeasy Mini Kit (Qiagen). After DNase treatment, cDNA was generated using an oligo$(dT)_{16}$ primer with SuperScript II reverse transcriptase (Invitrogen). Primer sequences for amplifying the coding region of the human *GALR1* cDNA (GenBank accession no. AY541036) are as follows: RT-*GALR1*-sense 5′-CACTTGCATAAAAAGTTGAAG-3′ (location in coding sequence; 676-696) and RT-*GALR1*-antisense 5′-TTATCACACATGAGTA-CAATTGG-3′ (1,053-1,031; ref. 30). The PCR product size was 378 bp. The PCR conditions were 94°C for 8 min; either 40 or 45 cycles at 94°C for 30 s, 52.0°C for 30 s, and 72°C for 45 s; and a final extension at 72°C for 8 min. Primers for the *GAPDH* gene were described previously (30).

Quantitative reverse transcription-PCR for GALR1. Quantitative PCR was done with the ABI PRISM 7700 HT Sequence Detection System (Applied Biosystems). Inventoried Assays-on-Demand Gene Expression Products (Applied Biosystems), which passed quality-control manufacturer's specifications, were used as primers and probe (Hs00175668_m1). The cDNA was generated from DNase-treated total RNA using Random primers (Invitrogen) with SuperScript II reverse transcriptase (Invitrogen). For each PCR evaluation, 10 μL diluted cDNA, 12.5 μL TaqMan Universal PCR Master Mix (Applied Biosystems), and 1.25 μL Assay Mix were added to a final volume of 25 μL. The thermal cycler conditions were as follows: 1 cycle of preheating at 50°C for 2 min and AmpliTaq Gold activation at 95°C for 10 min followed by 50 cycles of denaturing at 95°C for 15 s and annealing/extension at 60°C for 60 s. Analysis was done with ABI Prism Sequence Detection System v1.7a software (Applied Biosystems) following the manufacturer's instructions. For comparisons between samples, the mRNA expression of the target genes was normalized to *GAPDH* mRNA expression.

Immunohistochemistry. Tumor sections (5 μm) were dewaxed with xylene, hydrated through graded alcohols, and rehydrated in water. Sections were microwaved in citrate buffer (pH 6.0) three times for 5 min, and endogenous peroxidase activity was blocked using 0.5% hydrogen peroxide in methanol for 30 min. After a 20% goat serum was applied to the sections for 10 min, they were incubated with monoclonal antibodies against *cyclin D1* protein (1:100, 5D4; IBL),

Table 2. Multivariate analysis of factors influencing survival, determined by Cox's proportional hazards model

Variable	Relative risk (95% confidence interval)	*P*
Age		
≥70 vs <70	1.324 (0.692-2.533)	0.397
Smoking status		
Smoker vs nonsmoker	1.127 (0.560-2.270)	0.737
Tumor site		
Oral cavity and oropharynx vs others	0.786 (0.430-1.435)	0.433
Stage		
I, II, III vs IV	1.995 (1.044-3.811)	0.037*
Cyclin D1 expression		
High vs low	0.533 (0.223-1.270)	0.155
GALR1 methylation		
Yes vs no	2.515 (1.053-6.004)	0.038*

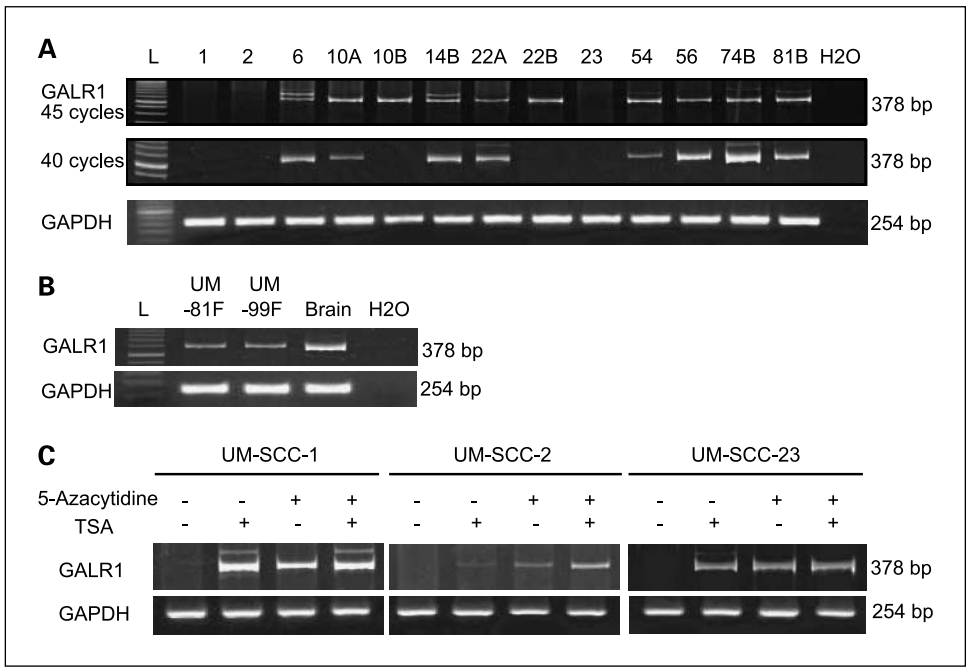

Fig. 2. GALR1 expression by RT-PCR. *A,* representative examples of RT-PCR for GALR1 expression in UM-SCC cell lines. PCR were carried out at 40 and 45 cycles to identify cell lines with low or absent GALR1 expression. The housekeeping gene GAPDH was run as a control for RNA integrity. *L,* 50-bp ladder in GALR1 and 100-bp ladder in GAPDH. *B,* representative examples of RT-PCR for GALR1 expression in nonmalignant samples. *C,* effect of treatment with 5-azacytidine, TSA, or both on GALR1 expression in three cell lines with densely methylated GALR1 is shown using RT-PCR. Controls were cells treated similarly but without 5-azacytidine or TSA.

p53 protein (1:1,000, Do7; DAKO), and *PTEN* (1:100, PN37; Invitrogen) at 4°C overnight (31).

Reactivation of GALR1 expression. Twelve hours after plating, cultures were incubated either for 48 h with 5-azacytidine (15 and 30 μg/mL; Sigma), an inhibitor of DNA methyltransferase, for 24 h with 300 nmol/L TSA (Sigma), an inhibitor of histone deacetylase, or for 48 h with 5-azacytidine followed by 24 h with TSA. The medium was then removed and cultures were maintained in standard DMEM, which was replaced every other day for 2 to 5 days. Transcripts were optimal on day 4 or 5 (32, 33).

Transient transfection, Western blotting, and cell proliferation assay. UM-SCC-23, a cell line established from a human laryngeal squamous cell carcinoma, was cultured in DMEM (Life Technologies) supplemented with 10% heat-inactivated fetal bovine serum at 37°C in 5% CO_2. The *GALR1* sequence was obtained from a human cDNA library (Invitrogen), COOH-terminal HA-tagged, and subcloned into the pcDNA3 vector (Invitrogen) containing an internal ribosomal entry site (Ires) and green fluorescent protein (GFP) sequence. The pCMVIresGFP vector was used as a transfection control. The UM-SCC-23-*GALR1* and UM-SCC-23-mock cells were established by transfecting with pCMVGALR1HAIresGFP or pCMVIresGFP respectively using LipofectAMINE (Invitrogen) followed by selection for GFP-positive cells. Twenty-four hours after plating, stably transfected cells were fed with serum-free medium containing 0.1% bovine serum albumin for 24 h to induce quiescence. Then, 1 μmol/L galanin (Anaspec) was added. Cell proliferation was measured by counting cells with a Coulter counter model Z1 (Beckman Coulter). Cells were lysed with 0.1% NP-40 lysis buffer containing protease (Calbiochem) and phosphatase (Sigma) inhibitor cocktails. To avoid protein aggregation, cells lysates were treated with 1,000 units *N*-glycosidase F or a mock digestion without the enzyme (mock; New England Biolabs) and subjected to electrophoresis without boiling. Equal amounts of protein were electrophoresed on 10% SDS-PAGE gels and transferred to Hybond-P (Amersham Biosciences). The mouse monoclonal anti-HA tag antibody (Convance) was used to detect exogenous *GALR1*. *GAPDH* was detected by mouse monoclonal anti-*GAPDH* (Chemicom International) as an internal control for protein loading. The membranes were incubated overnight with primary antibody at 4°C followed by incubation with horseradish peroxidase-conjugated rabbit anti-mouse secondary antibody (Amersham Biosciences).

Statistical analysis. The association between discrete variables and *GALR1* methylation was tested by the Fisher's exact probability test or the Mann-Whitney *U* test. In the colony formation assay, comparisons and tests for statistical significance were made by Student's *t* test. The 5-year overall survival rates were constructed using the method of Kaplan-Meier and analyzed by the log-rank test. Cox's proportional hazards regression analysis, which involved age, tumor site, smoking status, stage grouping, cyclin D1 expression, and *GALR1* methylation, was used to identify the multivariate predictive value of the prognostic factors. A significant difference was identified when the probability was <0.05.

Results

MSP. To determine if the *GALR1* promoter is affected by methylation in HNSCC, MSP analysis was carried out on bisulfite-treated DNA from 72 UM-SCC and UT-SCC cell lines as well as from fibroblast, EBV-transformed B lymphocyte, and normal keratinocyte samples. In addition, we analyzed bisulfite-treated DNA from primary tumors of 100 HNSCC patients in the Hamamatsu University Pathology archives. Forward primers for MSP and UMSP bind in the segment of the promoter that contains CpG dinucleotides 13 to 15, which correspond to a consensus Ap-2 site. Reverse primers for MSP and UMSP anneal to the segment that includes CpG dinucleotides 25 to 27, which correspond to a consensus Sp1 site (Fig. 1A). These sites are immediately upstream of the TSS. Examples of the methylated and unmethylated PCR products from a representative subset of the cell lines are shown in Fig. 1B and the results from all cell lines are summarized in Table 1. The subset included nine cell lines (UM-SCC-2, UM-SCC-10A, UM-SCC-10B, UM-SCC-14B, UM-SCC-22A, UM-SCC-22B, UM-SCC-23, UM-SCC-54, and UM-SCC-81B) shown previously to have LOH affecting the GALR1 locus, one with no 18q loss (UM-SCC-74B), and three (UM-SCC-1, UM-SCC-6, and UM-SCC-56) that were not tested for 18q loss. In three cell lines (UM-SCC-1, UM-SCC-2, and UM-SCC-23), only methylated

alleles were detected (Fig. 1B). Five other cell lines (UM-SCC-10B, UM-SCC-14B, UM-SCC-22B, UM-SCC-54, and UM-SCC-74B) had predominantly methylated alleles. In contrast, UM-SCC-81B, UM-SCC-10A, and UM-SCC-22A had only unmethylated alleles (Fig. 1B). Of interest, *GALR1* is mostly unmethylated in UM-SCC-10A and UM-SCC-22A, whereas *GALR1* is methylated in UM-SCC-10B and UM-SCC-22B that came from a recurrent and metastatic tumor, respectively. Among 72 UM-SCC and UT-SCC cell lines tested, the *GALR1* promoter was hypermethylated in 14 of 72 (19.4%) cases, partially methylated in 24 (33.3%), and unmethylated in 34 (47.2%). In contrast, 18 of 20 (90.0%) of the nonmalignant samples were unmethylated and only 2 (10.0%) were partially methylated (Supplementary Table S1). For comparison, we also assessed the methylation status of *p16* and *RASSF1A*, two tumor suppressor genes that are frequently reported to be silenced by methylation. As shown in Supplementary Table S1, like *GALR1*, *p16* was fully or partially methylated in 38% of the tumors and RASSF1A in 30%. Among DNA samples from 100 previously untreated primary tumors tested with the same primers (Fig. 1C), the *GALR1* promoter was methylated in 38 of 100 (38.0%) cases and unmethylated in 62 (62.0%). Methylation of *GALR1* significantly correlated with increased tumor size ($P = 0.0036$), lymph node status ($P = 0.0414$), tumor stage ($P = 0.0037$), increased *cyclin D1* expression ($P = 0.0420$), *p16* methylation ($P = 0.0494$), and overall 5-year survival ($P = 0.0448$; Table 1). There was no association with expression of p53, PTEN, or RASSAF1. In multivariate analysis, taking into account age, tumor site, smoking, tumor stage, and cyclin D1 expression, only *GALR1* methylation and stage were significant predictors of poor survival (Table 2).

***GALR1* expression in 13 UM-SCC cell lines tested for promoter methylation.** The 13 UM-SCC cell lines shown in Fig. 1 were tested for *GALR1* expression using reverse transcription-PCR (RT-PCR) with either 40 or 45 cycles of PCR. Absence of *GALR1* expression corresponded well with the methylation status shown in Fig. 1. Three cell lines (UM-SCC-1, UM-SCC-2, and UM-SCC-23) had no detectable *GALR1* mRNA even after 45 cycles as determined by absence of PCR product with this stringent test for message (Fig. 2A, *top*). cDNA from normal fibroblasts and brain were *GALR1* positive (Fig. 2B), which is consistent with *GALR1* expression in normal cells.

***GALR1* expression after 5-azacytidine and TSA treatment.** If DNA methylation and the associated deacetylation of histones that frequently accompanies methylation is responsible for silencing *GALR1* gene expression, it should be possible to reexpress the gene by reversing the epigenetic effects. We treated the three completely silenced cell lines (UM-SCC-1, UM-SCC-2, and UM-SCC-23) with methyltransferase (5-azacytidine) and/or histone deacetylase (TSA) inhibitors. In UM-SCC-1 and UM-SCC-23, either 5-azacytidine or TSA was sufficient to induce *GALR1* expression. For UM-SCC-2, only slight *GALR1* expression was observed when TSA was used alone. Given alone, 5-azacytidine induced some expression; however, when both drugs were used together *GALR1* expression was more robust. Thus, all three cell lines exhibited restored *GALR1* expression after inhibition of methyltransferase and histone deacetylase (Fig. 2C).

Bisulfite sequencing analysis. To examine the methylation of individual alleles and their association with GALR1 silencing, we focused on the 36 CpG sites surrounding the TSS (Fig. 1A) using BSP with the BSP primers for the top (BSP-U-F/BSP-U-RN/BSP-U-R) and bottom (BSP-L-F/BSP-L-R) DNA strands (as shown in Fig. 1A). We sequenced nine or more clones from the top and bottom strands of the DNA from 13 cell lines representing hypermethylated, partially methylated, or unmethylated examples. The percentage of methylated alleles for each of the 36 CpG sites is shown in Fig. 3A (top strand) and Fig. 3B (bottom strand) for the 13 HNSCC cell lines.

Methylation status of transcription factor binding sites. CpG sites 13 and 14 (top strand: 5′-GCC*CGCG*GC-3′ and bottom strand: 5′-GC*CGCG*GGC-3′) are within a near-perfect consensus AP-2 transcription factor binding site upstream of the TSS. DNA methylation within AP-2 binding sites is known to decrease the affinity of AP-2 binding (34). CpG site 26 is located within a consensus Sp1 binding site (top strand: 5′-GGG*CG*G-3′ and bottom strand: 5′-*CCG*CCC-3′). Transcription factor binding to Sp1 sites is also known to be significantly decreased by methylation of the first two cytosines on the bottom strand of the Sp1 recognition sequence (bottom strand: 5′-*CCG*CCC-3′; ref. 35). The frequency of methylated alleles corresponded to the MSP/UMSP results in Fig. 1 and with the amplification of message shown in Fig. 2.

Quantitative RT-PCR for GALR1. To quantify message expression in relation to promoter methylation generally and the transcription factor binding sites, real-time RT-PCR was used. The three *GALR1*-negative cell lines, UM-SCC-1, UM-SCC-2, and UM-SCC-23, are methylated on 100% of CpG sites 13, 14, and 26, with only two exceptions: UM-SCC-1 at site 14 (bottom strand) had 91% methylated alleles and UM-SCC-2 at site 13 (top strand) had 93% methylated alleles. A high proportion of these alleles are also heavily methylated in UM-SCC-10B, UM-SCC-14B, UM-SCC-22B, UM-SCC-54, and UM-SCC-74B, cell lines with barely detectable *GALR1* message. In contrast, for the cell lines with more readily detectable message, the proportion of heavily methylated alleles falls below 50% and the level of methylation at sites 13, 14, or 26 (Fig. 3A and B) also falls sharply with increasing message expression (Fig. 3C). In fact, in cell lines with readily detectable *GALR1* message expression, CpG sites 13 to 15 and 25 to 27 usually have only moderate methylation when compared with the nonexpressing hypermethylated cell lines. No *GALR1* message could be detected by quantitative PCR in cell lines UM-SCC-1, UM-SCC-2, and UM-SCC-23 ($\Delta\Delta$CT value: 0.029 + 0.031, 0.001 + 0.001, and 0.003 + 0.009; Fig. 3C). The average of the methylated alleles on the top and bottom strands in these cells lines was 94.8%, 95.0%, and 95.4%, respectively (Fig. 3A and B). UM-SCC-10B, UM-SCC-14B, UM-SCC-22B, UM-SCC-54, and UM-SCC-74B had barely detectable expression of *GALR1* by quantitative PCR ($\Delta\Delta$CT value: 0.051 + 0.023 to 0.182 + 0.023) and had a high proportion of methylated sites (averages: 88.8-92.7%). UM-SCC-6, UM-SCC-10A, UM-SCC-22A, UM-SCC-56, and UM-SCC-81B, which express *GALR1* expression by RT-PCR and quantitative PCR ($\Delta\Delta$CT value: 0.291 + 0.06 to 5.278 + 0.418), exhibited a range of methylation levels ranging from 2.8% to 43.2% of sequenced sites. Thus, promoter methylation showed considerable variability but was consistent with mRNA expression levels (Fig. 3C). To determine if *GALR1* methylation in tumor specimens also was associated with gene silencing, we isolated mRNA from frozen tissue. GALR1 expression analyzed by quantitative RT-PCR (Fig. 3D) showed that six tumors H-27,

H-40, H-52, H-63, H-72, and H-74 with strong methylation signals (Fig. 1C) exhibited little or no mRNA expression. In contrast, 3 of 6 (H-88, H-96, and H-97) tumors without *GALR1* promoter methylation (Fig. 1C) exhibited relatively robust mRNA expression (Fig. 3D).

Suppression of cell growth after restoration of GALR1 expression. UM-SCC-23 cell line, which exhibits extensive hypermethylation and expresses no GALR1 message, was used for assessment of exogenous GALR1 reexpression and effects on cell proliferation in response to galanin stimulation. UM-SCC-23 cells transfected with wild-type *GALR1* in the pCMVIresGFP or pCMV*GALR1*HAIresGFP constructs were assessed for GALR1 expression in Western blot using antibody specific for the HA tag (Fig. 4A). Treatment with 1 μmol/L galanin suppressed cell proliferation in UM-SCC-23GALR1HA cells by 24% (P = 0.0054) relative to the vector alone transfected cells

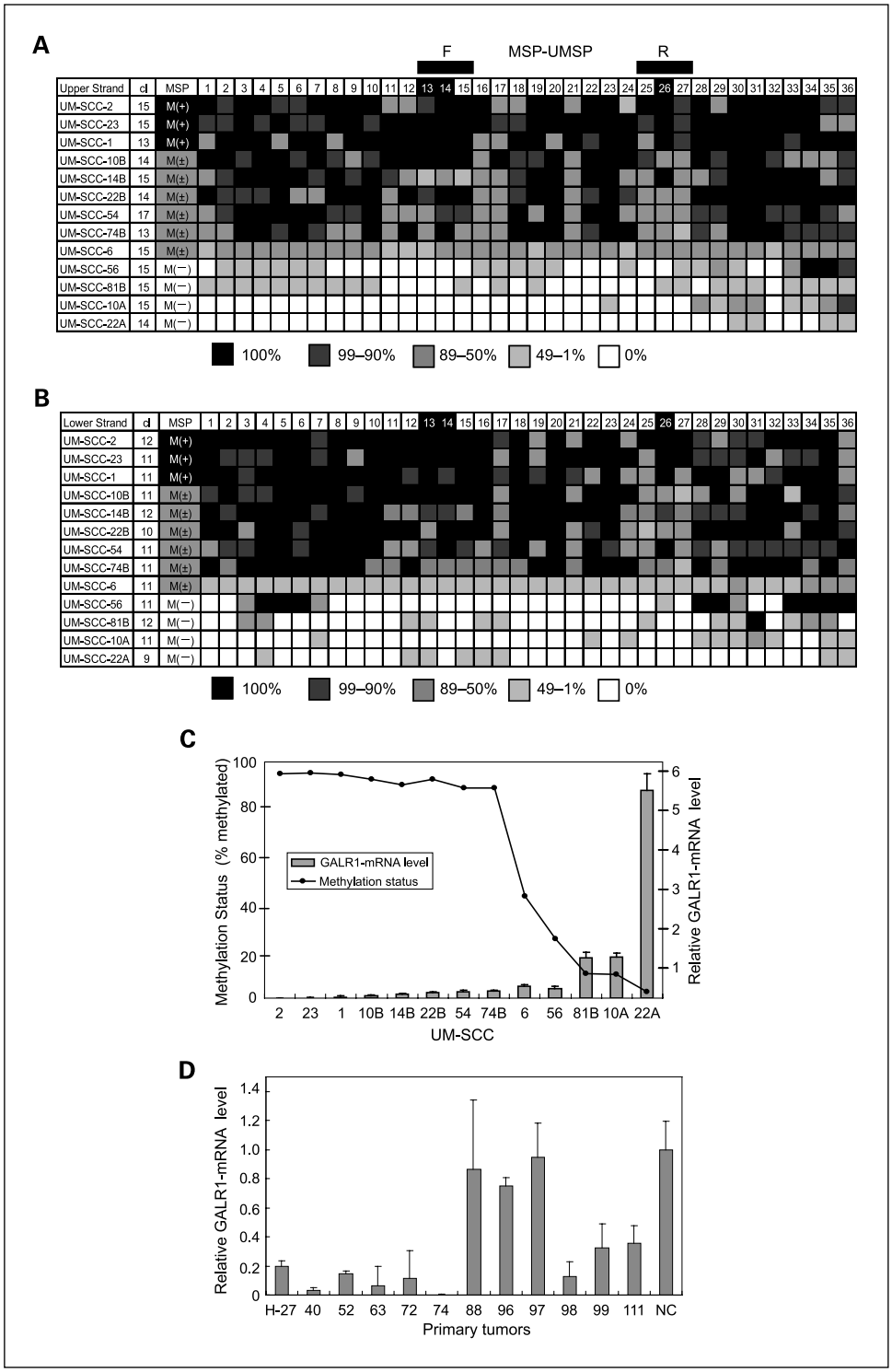

Fig. 3. Summary of bisulfite sequencing analysis and quantitative real-time PCR. *A,* bisulfite sequencing analysis of the top strand. *B,* bisulfite sequencing analysis of the bottom strand. The shading of each cell within the figure indicates the proportion of alleles that were found to be methylated by methylation-specific sequencing. The key is shown below each panel. *Numbers in the top row,* CpG dinucleotide positions (labeled 1-36 in Fig. 1) in the region amplified by the bisulfite sequencing (BSP) primers. The location of the MSP primer binding sites (MSP/UMSP-F and MSP/UMSP-R) used for the data in Fig. 1 are indicated by the *black boxes* above the figure. CpG sites 13, 14, and 26 are shaded in the top line to indicate that these sites are within the consensus transcription factor binding sites. *Left column,* cell line numbers; *second column,* number of clones sequenced (*cl*); *MSP column,* MSP results. *M* (+),positive for the GALR1-densely methylated form by MSP; *M* (±), some densely methylated and some unmethylated signal by MSP; *M(-),* negative for the GALR1-densely methylated form by MSP. *C,* comparison of methylation status and relative mRNA expression as assessed by quantitative RT-PCR of GALR1 in 13 UM-SCC cell lines. *D,* relative GALR1 mRNA expression as assessed by quantitative RT-PCR in 12 tumor specimens that were also evaluated for GALR1 promoter methylation. Specimens H-27, H-40, H-52, H-63, H-72, and H-74 exhibited promoter methylation, but H-88, H-96, H-97, H-99, and H-111 did not (Fig. 1C). *NC,* normal tissue control.

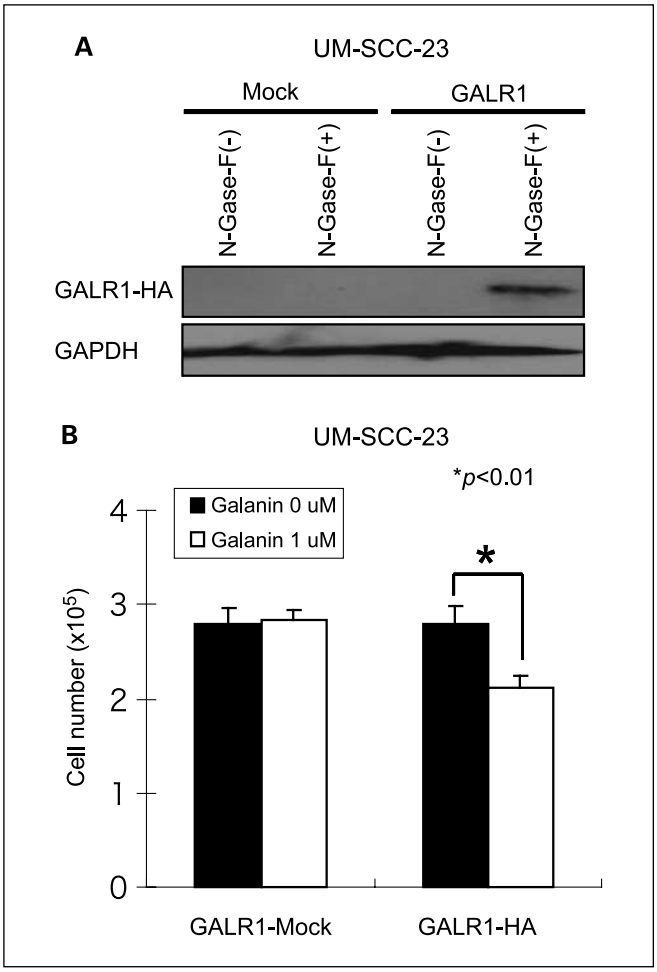

Fig. 4. Transient transfection, Western blotting, and cell proliferation assay. *A*, Western blot analysis shows exogenous GALR1 expression in pCMVGALR1HAIresGFP and pCMVIresGFP transfected cells with or without treatment with *N*-glycosidase F detected by antibody to the HA tag. *B*, relative colony formation ability for UM-SCC-23-GALR1 and UM-SCC-23-mock cells in response to treatment with galanin. In each case, the number of hygromycin B-resistant cells in vector-transfected controls was set at 100%. Cell proliferation was measured by counting cells with a Coulter counter model Z1. Mean ± SD of three separate experiments, each done in triplicate.

(Fig. 4B). Thus, *GALR1* inhibits tumor cell proliferation in response to galanin stimulation.

Discussion

Genetic analysis of HNSCC has revealed LOH at 3p, 8p, 9p, 11q, 13q, and 18q alleles in a significant fraction of tumors (36). 18q LOH is linked to advanced stage and poor survival in HNSCC, suggesting that one or more genes on this chromosome are important in tumor behavior (1). The commonly lost region of 18q is 18q23, which was lost in 53% (*D18S461*) to 75% (*D18S70*), including the *GALR1* locus (37). Galanin and its receptors are variably expressed in HNSCC (15).

GALR1 is a GPCR. GPCRs with the typical seven-transmembrane spanning domains and their ligands are involved in regulation of cellular physiology and complex behaviors mediated through numerous signal transduction and integration pathways (17, 38). We showed recently that, in HNSCC, galanin and GALR1 signal via extracellular signal-regulated kinase 1/2 activation to inhibit expression of cyclin D1, up-regulate expression of the cyclin-dependent kinase inhibitors $p27^{kip1}$ and $p57^{kip2}$, and inhibit tumor cell proliferation and tumor growth (22). These findings support the concept that *GALR1* regulates cell growth and functions as a tumor suppressor gene.

Some tumor suppressor genes exhibit homozygous loss, but in our studies of LOH, we found no examples of homozygous loss of the *GALR1* locus. Therefore, we suspected that an epigenetic mechanism of gene silencing might be at work. In this study, we show that GALR1 expression is frequently absent in HNSCC. Furthermore, expression-negative squamous cancers and cell lines exhibit hypermethylation of CpG islands in the *GALR1* promoter region. In a survey of 62 UM-SCC and 10 UT-SCC cell lines using *GALR1* promoter MSP, we showed that 14 of 72 (19.4%) were completely methylated and another 24 of 72 (33.3%) were partially methylated. Thus, more than half of the cell lines (52.7%) exhibit evidence of *GALR1* epigenetic silencing. The frequency of promoter methylation of *p16* 22 of 72 (30.6%) and *RASSF1A* 10 of 72 (13.9%), two other tumor suppressor genes, was similar to that of *GALR1* in the UM-SCC and UT-SCC cell lines. Hypermethylation of the *GALR1* promoter was also found in a similar proportion (38%) of primary head and neck tumor specimens, and suppression of GALR1 expression correlated with promoter methylation. Thus, *GALR1* resembles other major tumor suppressor genes in frequency of aberrant promoter methylation both *in vitro* and *in vivo*. Importantly, there is a significant correlation between *GALR1* promoter methylation and tumor size, lymph node status, tumor stage, *cyclin D1* expression, and *p16* methylation status in primary samples. Moreover, in multivariate analysis, only *GALR1* methylation and clinical stage were significantly associated with poor survival when age, smoking status, tumor site, and cyclin D1 expression were also considered. This is consistent with our earlier findings that LOH of the *GALR1* locus on 18q is associated with poor prognosis (1). Many lines with LOH had little or no GALR1 expression, which is consistent with loss of one allele and silencing of the other. We did find strong GALR1 expression in UM-SCC-74A, a cell line with no LOH. Of interest, LOH was present in primary tumor cell lines from two patients, UM-SCC-10A and UM-SCC-22A, but methylation was low or absent and GALR1 expression was still detectable. However, in the recurrent or metastatic tumor cell lines from these same donors, UM-SCC-10B and UM-SCC-22B, the methylation signal was potent, suggesting that silencing of the remaining allele occurred with progression. The significant association of increased cyclin D1 expression with GALR1 methylation in these tumors is consistent with our previous *in vitro* study (22) that showed that GALR1 and galanin down-regulate cyclin D1 expression. Thus, loss of *GALR1* expression appears to be linked to loss of control of cyclin D1 expression, which is consistent with tumor progression.

The MSP assay is a convenient and sensitive method to examine promoter methylation status, and in this study, it was fully concordant with mRNA expression. It became clear that although these cell lines have a strong promoter methylation signal, a critical feature in complete suppression of mRNA expression is whether the transcription factor binding sites are hypermethylated. Thus, the choice of the correct primer sets is

an essential element for an effective MSP assay and should be designed based on bisulfite-treated DNA sequencing and mRNA expression (39, 40) as we did in the current study. The MSP and UMSP each included three CpG sites, which spanned at least two transcription factor binding sites. AP-2 is a cell type-specific transcription factor expressed in neural crest and ectoderm-derived tissues, including craniofacial, skin, and urogenital tissues. Although footprinting has shown some promiscuity in AP-2 sites, AP-2 protein homodimers bind consistently to a consensus palindromic sequence, 5′-GCCNNNGGC-3′. In the *GALR1* promoter, this sequence includes CpG sites 13 and 14 (41, 42). AP-2 has roles in both normal development and development/progression of cancer (42). Methylation at CpGs within the AP-2-binding site distinguish the UM-SCC cell lines (such as UM-SCC-1, UM-SCC-2, and UM-SCC-23) that fail to express *GALR1* mRNA from those such as UM-SCC-14B and UM-SCC-74B that do express *GALR1*. This is consistent with reports indicating that methylation of AP-2 CpG sites inhibits AP-2 binding and suppresses AP-2-regulated transcription of genes such as *SOD2*, *E-cadherin*, and the *proenkephalin-CAT* gene (34, 43, 44). Sp1 sites are found in the promoter region of many housekeeping genes, indicating a role for the Sp1 as a basal transcription factor (45). Some reports indicate that methylation at Sp1 binding sites has no influence on Sp1 binding (35, 46), whereas others (28) used electrophoretic mobility shift assays to show that Sp1 binding to the *Rb* promoter can be abolished when the first two cytosines on the bottom strand (5′-*CCG*CCC-3′) are methylated (34). Similarly, the MBD1 and MCAF complex blocks transcription by affecting Sp1 in heavily methylated promoter regions (47). MCAF physically binds Sp1 and the general transcription apparatus like a positive regulator. MBD1-MCAF seems to interfere with Sp1-mediated activation of the transcription preinitiation complexes in methylated DNA regions (47). The methyl groups on DNA could interfere with binding of specific transcription factors and have been described as a mechanism for transcriptional inactivation of tumor suppressor genes in subsets of primary cancers. Within the CpG islands, there is typically a core promoter and a TSS and gene expression is completely repressed when this region becomes hypermethylated (48). Our results show that the methylation levels of CpG sites 13 and 14, on the top strand in the AP-2 binding site, strongly influence the expression of *GALR1* mRNA. In addition, it is likely that heavy methylation of the promoter region also causes inhibition of Sp1 binding and repression of *GALR1* mRNA expression.

Furthermore, in 3 of 3 HNSCC cell lines that do not express any detectable *GALR1* mRNA, the gene could be reactivated by treatment with 5-azacytidine alone, TSA alone, and/or the combination of 5-azacytidine and TSA. Reactivation of heavily methylated cell lines with histone deacetylase inhibitors alone is somewhat unusual and indicates that chromatin silencing effects can be reversed even in the presence of DNA methylation. This also suggests that the combination of methylation and deacetylation act together to silence expression and that variability in DNA acetylation may account for some of the heterogeneity we observed in expression of *GALR1* in lines with relatively strong methylation signals. Our data show that in HNSCC promoter hypermethylation of *GALR1* is associated with loss of gene expression that can be reversed by treatment with methyltransferase and histone deacetylase inhibitors.

Our results are consistent with the hypothesis that *GALR1* is a probable tumor suppressor gene in HNSCC. We show for the first time that expression of *GALR1* mRNA is lost in HNSCC as a consequence of DNA methylation. Furthermore, silencing of the *GALR1* gene by methylation may be a critical event in tumor progression of HNSCC, because 18q LOH is associated with tumor progression (36), and in this study, *GALR1* promoter methylation was observed to be greater in cell lines derived from secondary tumors in the same patient (e.g., UM-SCC-10A has a weaker MSP signal than UM-SCC-10B), and the same occurs in UM-SCC-22A and UM-SCC-22B. Furthermore, *GALR1* promoter methylation was associated with larger primary tumor size, clinical stage, lymph node metastasis, *cyclin D1* expression and *p16* methylation, and poorer survival. In this article, we have shown that transcriptional repression is likely mediated by inhibition of AP-2 and Sp1 binding secondary to methylation of critical CpGs in the *GALR1* promoter. Furthermore, reexpression of GALR1 in transfected cells results in galanin-induced inhibition of cell proliferation. Finally, *GALR1* can be reactivated by altering chromatin modifications with methyltransferase and histone deacetylase inhibitors, raising the promise of selective small-molecule inhibitors of these enzymes as potential therapeutic agents in HNSCC.

Disclosure of Potential Conflicts of Interest

No potential conflicts of interest were disclosed.

Acknowledgments

We thank Prof. Mitsuyoshi Nakao (Department of Regeneration Medicine, Institute of Molecular Embryology and Genetics, Kumamoto University) and Prof. Keith Kirkwood (Department of Periodontics and Oral Medicine at the University of Michigan) for helpful advice.

References

1. Pearlstein RP, Benninger MS, Carey TE, et al. Loss of 18q predicts poor survival of patients with squamous cell carcinoma of the head and neck. Genes Chromosomes Cancer 1998;21:333–9.
2. Takebayashi S, Ogawa T, Jung KY, et al. Identification of new minimally lost regions on 18q in head and neck squamous cell carcinoma. Cancer Res 2000;60:3397–403.
3. Taborga M, Corcoran KE, Fernandes N, Ramkissoon SH, Rameshwar P. G-coupled protein receptors and breast cancer progression: potential drug targets. Mini Rev Med Chem 2007;7:245–51.
4. Touge H, Chikumi H, Igishi T, et al. Diverse activation states of RhoA in human lung cancer cells: contribution of G protein coupled receptors. Int J Oncol 2007;30:709–15.
5. Spiegelberg BD, Hamm HE. Roles of G-protein-coupled receptor signaling in cancer biology and gene transcription. Curr Opin Genet Dev 2007;17:40–4.
6. Cheng Y, Lotan R. Molecular cloning and characterization of a novel retinoic acid-inducible gene that encodes a putative G protein-coupled receptor. J Biol Chem 1998;273:35008–15.
7. Gschwind A, Prenzel N, Ullrich A. Lysophosphatidic acid-induced squamous cell carcinoma cell proliferation and motility involves epidermal growth factor receptor signal transactivation. Cancer Res 2002;62:6329–36.
8. Henson BS, Neubig RR, Jang I, et al. Galanin receptor

1 has anti-proliferative effects in oral squamous cell carcinoma. J Biol Chem 2005;280:22564–71.
9. Lin R, Nagai Y, Sladek R, et al. Expression profiling in squamous carcinoma cells reveals pleiotropic effects of vitamin D_3 analog EB1089 signaling on cell proliferation, differentiation, and immune system regulation. Mol Endocrinol 2002;16:1243–56.
10. Rhee CS, Sen M, Lu D, et al. Wnt and frizzled receptors as potential targets for immunotherapy in head and neck squamous cell carcinomas. Oncogene 2002;21:6598–605.
11. Thomas SM, Bhola NE, Zhang Q, et al. Cross-talk between G protein-coupled receptor and epidermal growth factor receptor signaling pathways contributes to growth and invasion of head and neck squamous cell carcinoma. Cancer Res 2006;66:11831–9.
12. Zhang Q, Thomas SM, Lui VW, et al. Phosphorylation of TNF-α converting enzyme by gastrin-releasing peptide induces amphiregulin release and EGF receptor activation. Proc Natl Acad Sci U S A 2006;103:6901–6.
13. Zhang Q, Thomas SM, Xi S, et al. SRC family kinases mediate epidermal growth factor receptor ligand cleavage, proliferation, and invasion of head and neck cancer cells. Cancer Res 2004;64:6166–73.
14. Zhang X, Hunt JL, Landsittel DP, et al. Correlation of protease-activated receptor-1 with differentiation markers in squamous cell carcinoma of the head and neck and its implication in lymph node metastasis. Clin Cancer Res 2004;10:8451–9.
15. Ogawa T, Ogawa H, Ueda Y, et al. Expression and mutation of galanin receptor 1 in head and neck squamous cell carcinoma (HNSCC) cell lines. In: Proc AACR; 2001. p. 621.
16. Wang S, Hashemi T, Fried S, Clemmons AL, Hawes BE. Differential intracellular signaling of the GalR1 and GalR2 galanin receptor subtypes. Biochemistry 1998;37:6711–7.
17. Branchek TA, Smith KE, Gerald C, Walker MW. Galanin receptor subtypes. Trends Pharmacol Sci 2000;21:109–17.
18. Gundlach AL. Galanin/GALP and galanin receptors: role in central control of feeding, body weight/obesity and reproduction? Eur J Pharmacol 2002;440:255–68.
19. Bartfai T, Fisone G, Langel U. Galanin and galanin antagonists: molecular and biochemical perspectives. Trends Pharmacol Sci 1992;13:312–7.
20. Wittau N, Grosse R, Kalkbrenner F, Gohla A, Schultz G, Gudermann T. The galanin receptor type 2 initiates multiple signaling pathways in small cell lung cancer cells by coupling to G(q), G(i) and G(12) proteins. Oncogene 2000;19:4199–209.
21. Berger A, Lang R, Moritz K, et al. Galanin receptor subtype GalR2 mediates apoptosis in SH-SY5Y neuroblastoma cells. Endocrinology 2004;145:500–7.
22. Kanazawa T, Iwashita T, Kommareddi P, et al. Galanin and galanin receptor type 1 suppress proliferation in squamous carcinoma cells: activation of the extracellular signal regulated kinase pathway and induction of cyclin-dependent kinase inhibitors. Oncogene 2007;26:5762–71.
23. Suzuki K, Suzuki I, Leodolter A, et al. Global DNA demethylation in gastrointestinal cancer is age dependent and precedes genomic damage. Cancer Cell 2006;9:199–207.
24. Iismaa TP, Fathi Z, Hort YJ, et al. Structural organization and chromosomal localization of three human galanin receptor genes. Ann N Y Acad Sci 1998;863:56–63.
25. Baylin SB, Ohm JE. Epigenetic gene silencing in cancer—a mechanism for early oncogenic pathway addiction? Nat Rev 2006;6:107–16.
26. Verma M, Srivastava S. Epigenetics in cancer: implications for early detection and prevention. Lancet Oncol 2002;3:755–63.
27. Park NH, Min BM, Li SL, Huang MZ, Cherick HM, Doniger J. Immortalization of normal human oral keratinocytes with type 16 human papillomavirus. Carcinogenesis 1991;12:1627–31.
28. Herman JG, Graff JR, Myohanen S, Nelkin BD, Baylin SB. Methylation-specific PCR: a novel PCR assay for methylation status of CpG islands. Proc Natl Acad Sci U S A 1996;93:9821–6.
29. Kuroki T, Trapasso F, Yendamuri S, et al. Allele loss and promoter hypermethylation of VHL, RAR-β, RASSF1A, and FHIT tumor suppressor genes on chromosome 3p in esophageal squamous cell carcinoma. Cancer Res 2003;63:3724–8.
30. Berger A, Tuechler C, Almer D, et al. Elevated expression of galanin receptors in childhood neuroblastic tumors. Neuroendocrinology 2002;75:130–8.
31. Mineta H, Miura K, Takebayashi S, et al. Cyclin D1 overexpression correlates with poor prognosis in patients with tongue squamous cell carcinoma. Oral Oncol 2000;36:194–8.
32. Cheung JO, Grant ME, Jones CJ, Hoyland JA, Freemont AJ, Hillarby MC. Apoptosis of terminal hypertrophic chondrocytes in an *in vitro* model of endochondral ossification. J Pathol 2003;201:496–503.
33. Wada M, Yazumi S, Takaishi S, et al. Frequent loss of RUNX3 gene expression in human bile duct and pancreatic cancer cell lines. Oncogene 2004;23:2401–7.
34. Huang Y, Peng J, Oberley LW, Domann FE. Transcriptional inhibition of manganese superoxide dismutase (SOD2) gene expression by DNA methylation of the 5′ CpG island. Free Radic Biol Med 1997;23:314–20.
35. Clark SJ, Harrison J, Molloy PL. Sp1 binding is inhibited by (m)Cp(m)CpG methylation. Gene 1997;195:67–71.
36. Van Dyke DL, Worsham MJ, Benninger MS, et al. Recurrent cytogenetic abnormalities in squamous cell carcinomas of the head and neck region. Genes Chromosomes Cancer 1994;9:192–206.
37. Takebayashi S, Hickson A, Ogawa T, et al. Loss of chromosome arm 18q with tumor progression in head and neck squamous cancer. Genes Chromosomes Cancer 2004;41:145–54.
38. Gutkind JS. Cell growth control by G protein-coupled receptors: from signal transduction to signal integration. Oncogene 1998;17:1331–42.
39. Dote H, Toyooka S, Tsukuda K, et al. Aberrant promoter methylation in human DAB2 interactive protein (hDAB2IP) gene in breast cancer. Clin Cancer Res 2004;10:2082–9.
40. Toyooka S, Toyooka KO, Harada K, et al. Aberrant methylation of the CDH13 (H-cadherin) promoter region in colorectal cancers and adenomas. Cancer Res 2002;62:3382–6.
41. Williams T, Tjian R. Analysis of the DNA-binding and activation properties of the human transcription factor AP-2. Genes Dev 1991;5:670–82.
42. Tellez C, Bar-Eli M. Role and regulation of the thrombin receptor (PAR-1) in human melanoma. Oncogene 2003;22:3130–7.
43. Xu Y, Porntadavity S, St Clair DK. Transcriptional regulation of the human manganese superoxide dismutase gene: the role of specificity protein 1 (Sp1) and activating protein-2 (AP-2). Biochem J 2002;362:401–12.
44. Comb M, Goodman HM. CpG methylation inhibits proenkephalin gene expression and binding of the transcription factor AP-2. Nucleic Acids Res 1990;18:3975–82.
45. Zou MX, Butcher DT, Sadikovic B, Groves TC, Yee SP, Rodenhiser DI. Characterization of functional elements in the neurofibromatosis (NF1) proximal promoter region. Oncogene 2004;23:330–9.
46. Mancini DN, Singh SM, Archer TK, Rodenhiser DI. Site-specific DNA methylation in the neurofibromatosis (NF1) promoter interferes with binding of CREB and SP1 transcription factors. Oncogene 1999;18:4108–19.
47. Fujita N, Watanabe S, Ichimura T, et al. MCAF mediates MBD1-dependent transcriptional repression. Mol Cell Biol 2003;23:2834–43.
48. Nakao M. Epigenetics: interaction of DNA methylation and chromatin. Gene 2001;278:25–31.